Neutrino oscillation anomalies

Christoph Andreas Ternes[1,2*]

[1]Istituto Nazionale di Fisica Nucleare (INFN), Sezione di Torino, Via P. Giuria 1, I–10125 Torino, Italy
[2]Dipartimento di Fisica, Università di Torino, via P. Giuria 1, I–10125 Torino, Italy

Abstract. I give an overview of some of the several anomalies appearing in neutrino oscillation experiments, setting particular focus to the reactor antineutrino anomaly and the Gallium anomaly. I will discuss these two anomalies in some detail and, in particular, compare their explanation due to neutrino oscillations in presence of a light sterile neutrino among each other and also with the bounds from the analyses of reactor spectral ratio data, β-decay data, and solar neutrino data.

1 Introduction

The possible existence of light sterile neutrinos is a hot topic of current research in high-energy physics. It was motivated by anomalies found in short-baseline neutrino oscillation experiments: the Gallium Anomaly, the Reactor Antineutrino Anomaly, and the LSND and MiniBooNE anomalies (see the reviews in Refs. [1–4]). Most puzzling is the large Gallium Anomaly, which has been recently revived by the results of the BEST experiment [5, 6]. Here, we discuss the status of short-baseline ν_e and $\bar{\nu}_e$ disappearance and we compare the neutrino oscillation explanation of the Gallium Anomaly with the constraints from other experiments.

The standard paradigm in the phenomenology of massive neutrinos is the three-neutrino mixing scheme in which the three well known active flavor neutrinos ν_e, ν_μ, and ν_τ take part in the weak interactions of the Standard Model and are unitary superpositions of three massive neutrinos ν_1, ν_2, and ν_3 with respective masses m_1, m_2, and m_3. The two independent squared-mass differences $\Delta m^2_{21} \approx 7.4 \times 10^{-5}\,\text{eV}^2$ and $|\Delta m^2_{31}| \approx 2.5 \times 10^{-3}\,\text{eV}^2$ (with $\Delta m^2_{kj} \equiv m^2_k - m^2_j$) generate the oscillations observed in solar, atmospheric and long-baseline neutrino oscillation experiments (see for example Ref. [7]). Short-baseline (SBL) oscillations that could explain the Reactor Antineutrino Anomaly and the Gallium Anomaly require the existence of at least one additional squared-mass difference $\Delta m^2_{\text{SBL}} \gtrsim 1\,\text{eV}^2$. In the minimal 3+1 scenario that we consider here there is a non-standard massive neutrino ν_4 with mass $m_4 \gtrsim 1\,\text{eV}$ which generates the short-baseline squared-mass difference $\Delta m^2_{\text{SBL}} \simeq \Delta m^2_{41}$. In the flavor basis, the new neutrino corresponds to a sterile neutrino ν_s which does not take part in the weak interactions of the Standard Model (see the reviews in Refs. [1–4]). In this framework, the effective short-baseline survival probability of electron neutrinos and antineutrinos relevant for reactor and Gallium experiments is given by $P_{ee} \simeq 1 - \sin^2 2\vartheta_{ee} \sin^2\left(\frac{\Delta m^2_{41} L}{4E}\right)$. The effective mixing angle ϑ_{ee} depends on the element U_{e4} of the 4×4 mixing matrix U through the relation $\sin^2 2\vartheta_{ee} = 4|U_{e4}|^2(1 - |U_{e4}|^2)$.

Currently, the Reactor Antineutrino Anomaly is regarded to be resolved or, at least, diminished with the new refinements of reactor flux models [8, 9], but the Gallium Anomaly is reinforced by the new measurements of the BEST experiment [5, 6]. Therefore, it is desirable to pay special attention to the Gallium Anomaly, and look for possible viable solutions.

2 The Gallium Anomaly

The Gallium Anomaly was originally [10–12] a deficit of events observed in the GALLEX [13–15] and SAGE [10, 16–18] source experiments aimed at testing the solar neutrino detection done in these experiments through the process $\nu_e + {}^{71}\text{Ga} \to e^- + {}^{71}\text{Ge}$. Two source experiments have been done by the GALLEX collaboration using an intense artificial ^{51}Cr radioactive source placed inside the detector. This source emitted electron neutrinos through the electron capture (EC) process $e^- + {}^{51}\text{Cr} \to {}^{51}\text{V} + \nu_e$. The SAGE collaboration performed a source experiment with a ^{51}Cr radioactive source and another with a ^{37}Ar radioactive source, which emitted electron neutrinos through the EC process $e^- + {}^{37}\text{Ar} \to {}^{37}\text{Cl} + \nu_e$. The deficits of the observed rates with respect to the rates calculated from the well-measured activity of the sources and different cross sections for the detection process have been discussed in many papers. The measurements from GALLEX and SAGE have been recently confirmed in the BEST experiment [5, 6], which was using also a ^{51}Cr radioactive source.

The determination of the significance of the Gallium anomaly depends on the theoretical prediction of the detection cross section for which there are several model calculations. The difference between these cross section models is the contribution to the cross section coming

*ternes@to.infn.it

from the transitions from the ground state of ^{71}Ga to excited states of ^{71}Ge. The ground-state to ground-state cross section is known with a very small uncertainty from the measured lifetime of ^{71}Ge [19], whereas the transitions to the excited states are obtained from theoretical calculations. These relative contributions are expected to be at the few % level, with the exact value depending on the cross section model. The cross section models that we consider here are a "Ground-state model" where no contribution from the excited states is considered and the calculations from Bahcall [19], Kostensalo et al. [20] and Semenov [21]. It has been shown that the statistical significance of the Gallium Anomaly is large, about 5-6σ, for all the cross section models [22, 23]. The Gallium Anomaly can be explained by short-baseline neutrino oscillations in the 3+1 active-sterile neutrino mixing framework described briefly in Section 1. Fig. 1 shows the 2σ allowed regions in the $(\sin^2 2\vartheta_{ee}, \Delta m^2_{41})$ plane obtained from the analyses of the Gallium data with the different cross section models. One can see that in all cases there is a clear indication of a relatively large value of $\sin^2 2\vartheta_{ee}$ for $\Delta m^2_{41} \gtrsim 0.6\,\mathrm{eV}^2$. The minimum 2σ value of $\sin^2 2\vartheta_{ee}$ is about 0.14 in the case of the Ground State model. For the other cross section models the allowed regions lie at even larger values of $\sin^2 2\vartheta_{ee}$. The Kostensalo Shell Model cross section requires values of $\sin^2 2\vartheta_{ee}$ that are only slightly larger than those of the Ground State cross section, $\sin^2 2\vartheta_{ee} \gtrsim 0.17$, because of the small contribution of the transitions to the excited states of ^{71}Ge in this cross section model. The Bahcall cross section implies $\sin^2 2\vartheta_{ee} \gtrsim 0.17$, and the Semenov cross sections give $\sin^2 2\vartheta_{ee} \gtrsim 0.23$.

3 The reactor rates constraints

The phenomenology of reactor neutrinos focused on the Reactor Antineutrino Anomaly in 2011 [24], after the reevaluations of the predicted reactor antineutrino fluxes by Mueller *et al.* [25] and Huber [26] (HM model), which led to a deficit of about 2.5σ of observed event rates in short-baseline reactor neutrino experiments with respect to the predictions. Recent theoretical and experimental developments led to new reactor flux models with enhanced (HKSS model of Hayen, Kostensalo, Severijns, and Suhonen [27]) or diminished (EF model of Estienne, Fallot *et al* [28] and KI model of Kopeikin *et al.* [29]) Reactor Antineutrino Anomaly. In particular, the EF and KI flux models give average ratios of observed and predicted events that are only about 1σ smaller than unity, hinting at the demise of the Reactor Antineutrino Anomaly [8, 9]. Here we use the results of the analysis in Ref. [9], where it was shown that all the reactor flux models imply upper bounds for the 3+1 active-sterile neutrino mixing parameter $\sin^2 2\vartheta_{ee}$ that are smaller than about 0.25 at 2σ. This bound is in tension with the large values of $\sin^2 2\vartheta_{ee}$ which are required to explain the Gallium Anomaly, as discussed in Section 2.

Figure 1 shows a comparison of the 2σ allowed regions in the $(\sin^2 2\vartheta_{ee}, \Delta m^2_{41})$ plane obtained from the analyses of reactor rates and Gallium data. One can see that there is only a small overlap of the reactor and Gallium regions for some models.

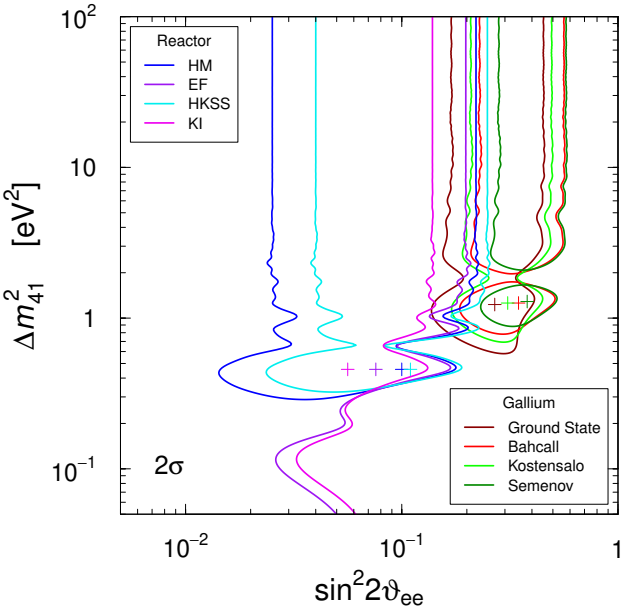

Figure 1. Contours delimiting the 2σ allowed regions in the $(\sin^2 2\vartheta_{ee}, \Delta m^2_{41})$ plane obtained from the Gallium data with different cross sections compared with those obtained in Ref. [9] from the analysis of short-baseline reactor rate data. The best-fit points are indicated by crosses.

Table 2 of Ref. [22] shows the χ^2 difference $\Delta\chi^2_{\mathrm{PG}}$ of the parameter goodness of fit test [30] between the reactor rates and the Gallium data corresponding to the models in Fig. 1. Also shown are the corresponding values of the parameter goodness of fit $\mathrm{GoF}_{\mathrm{PG}}$, which quantifies the tension between the fits of reactor rates and Gallium data in the different models. Considering the extreme case of Ground State Gallium cross section model, the largest tension is obtained with the KI reactor flux model ($\mathrm{GoF}_{\mathrm{PG}} = 0.26\%$). Indeed, one can see from Fig. 1 that the corresponding 2σ allowed regions have only a very marginal overlap for $\Delta m^2_{41} \simeq 1\,\mathrm{eV}^2$.

The more realistic Bahcall, Kostensalo, and Semenov cross section models give larger tensions between the reactor rates and Gallium data. If we consider as severe a tension with a $\mathrm{GoF}_{\mathrm{PG}}$ smaller than 1%, for the Bahcall and Kostensalo cross section models there is a severe tension between Gallium data and reactor rates for all reactor flux models, except the HKSS model, while for the Semenov cross section model there is a severe tension for all of the reactor flux models. One can also notice that the KI reactor flux model gives the maximal tension for all Gallium cross section models and it is always severe. The EF reactor flux model gives a severe tension for all the Gallium cross section models, except for the Ground State model, where it is a marginal 1.1%.

Since the EF and KI reactor flux models are those that may have solved the Reactor Antineutrino Anomaly and are currently believed to represent reliable replacements of the standard HM model, we conclude that the tension

between Gallium data and reactor rates is a serious issue in the framework of 3+1 active-sterile neutrino oscillations.

4 Short-baseline reactor spectral ratios

Short-baseline oscillations of reactor antineutrinos can be probed in a model-independent way by comparing the rates or spectra measured at different distances from the reactor antineutrino source. This is the approach adopted by the recent DANSS [31, 32], PROSPECT [33, 34], and STEREO [35, 36] experiments. Important results have been obtained also by the NEOS collaboration [37] and by a joint analysis of the RENO and NEOS collaborations [38]. In 2017 [37] the NEOS collaboration published the results of the comparison of NEOS data at about 24 m from the reactor source with the prediction obtained from the neutrino flux measured in the Daya Bay experiment [39] at a distance of about 550 m from the reactor source, where the short-baseline oscillations are averaged. Recently, the RENO and NEOS collaborations published a joint paper [38] with the results of the comparison of NEOS data with the prediction obtained from the neutrino flux measured in the RENO experiment at a distance of about 419 m from the reactor source, which is in the same reactor complex of NEOS. This comparison allowed the RENO and NEOS collaborations to reduce the systematic uncertainties with respect to the NEOS/Daya Bay analysis.

In the following we consider both the NEOS/Daya Bay and NEOS/RENO data, because it is obviously unknown which one of the Daya Bay and RENO neutrino spectra is more accurate. Note that in this analysis we do not consider the controversial results of the Neutrino-4 experiment: the Neutrino-4 collaboration claimed a 2.9σ evidence of short-baseline neutrino oscillations with large mixing ($\sin^2 2\vartheta_{ee} = 0.36 \pm 0.12$) at $\Delta m^2_{41} = 7.3 \pm 1.17$ [40]. However, these results were criticized in Refs. [41–44].

In the following we discuss the compatibility of the results of the fits of reactor spectral ratio data with the neutrino oscillation interpretation of the Gallium data and we perform combined fits with other experimental results. For convenience, we introduce the following notation:

RSRF(N/DB) combined reactor spectral ratio fit of the NEOS/Daya Bay, DANSS, PROSPECT, STEREO, and Bugey-3 data.

RSRF(N/R) combined reactor spectral ratio fit of the NEOS/RENO, DANSS, PROSPECT, STEREO, and Bugey-3 data.

As shown in Fig. 2, these combined fits of the data of reactor spectral ratio experiments favor short-baseline neutrino oscillations at values of Δm^2_{41} which are compatible with the neutrino oscillation interpretation of the Gallium data discussed in Section 2, but the required values of the mixing angle are smaller. Therefore, there is again a tension between the results of reactor spectral ratio experiments and those of the Gallium experiments. For all the four Gallium detection cross section models, the parameter goodness of fit is well below 1% for RSRF(N/DB),

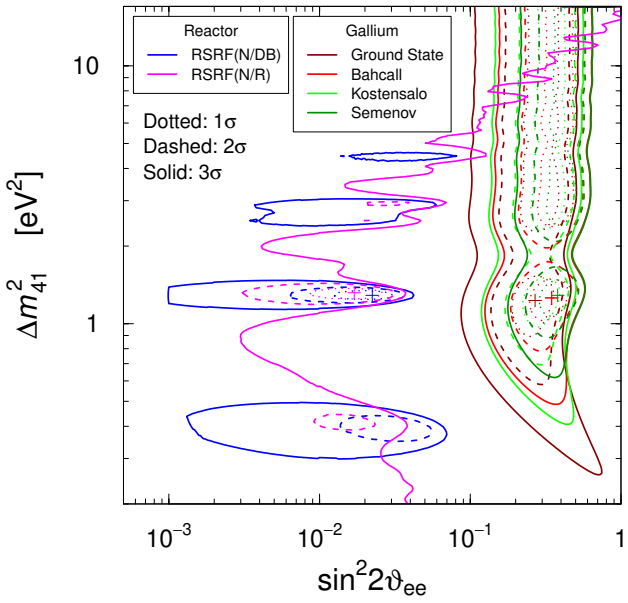

Figure 2. Contours delimiting the 1σ, 2σ, and 3σ allowed regions in the $(\sin^2 2\vartheta_{ee}, \Delta m^2_{41})$ plane obtained from the Gallium data with different cross sections compared with those obtained from the two analyses of reactor spectral ratio data discussed in the text. The best-fit points are indicated by crosses.

whereas it is slightly above 1% for RSRF(N/R) as indicated in Tab. 3 of Ref. [22]. The larger compatibility of RSRF(N/R) with the Gallium data may seem contradictory with the smaller statistical significance of short-baseline neutrino oscillations of RSRF(N/R) (2.6σ) with respect to RSRF(N/DB) (3.1σ). However, one can see from Fig. 2 that the 3σ allowed region of RSRF(N/R) extends to large values of $\sin^2 2\vartheta_{ee}$ for large values of Δm^2_{41}, leading to a relative compatibility with the Gallium allowed regions. On the other hand, the 3σ allowed regions of RSRF(N/DB) are closed and lie at values of $\sin^2 2\vartheta_{ee}$ that are incompatible with the Gallium allowed regions.

5 Global ν_e and $\bar{\nu}_e$ disappearance analysis

In this Section we present the results of the global analysis of the ν_e and $\bar{\nu}_e$ disappearance data in the framework of 3+1 active-sterile neutrino mixing. The data that we consider are the reactor rates and the reactor spectral ratio data discussed above. We include also the Tritium limits and the solar bound discussed in detail in Ref. [22]. We will discuss the global tension between the data that we consider and the Gallium data if the Gallium Anomaly is considered as due to 3+1 active-sterile neutrino mixing. Since the tension is very strong, we cannot include the Gallium data in a global fit in the framework of 3+1 active-sterile neutrino mixing, and we presume that the Gallium Anomaly is due to other reasons.

The results of the global fits that we obtained with different data sets (NEOS/Daya Bay or NEOS/RENO) and different reactor flux models are listed in Tab. 1. One can see that the goodness of fit is high. There is a 3.1–3.3σ

	Global RSRF(N/DB) Fit			
	HM	HKSS	EF	KI
$\chi^2_{\rm min}$	393.5	395.2	391.2	391.4
GoF	43%	40%	46%	46%
$(\sin^2 2\vartheta_{ee})_{\rm b.f.}$	0.022	0.022	0.022	0.022
$(\Delta m^2_{41})_{\rm b.f.}/{\rm eV}^2$	1.29	1.29	1.29	1.29
$\Delta\chi^2_{4\nu\text{-}3\nu}$	13.8	14.1	12.6	12.9
$n\sigma_{4\nu\text{-}3\nu}$	3.3	3.3	3.1	3.2
	Global RSRF(N/R) Fit			
	HM	HKSS	EF	KI
$\chi^2_{\rm min}$	386.5	388.3	384.0	384.2
GoF	53%	50%	56%	56%
$(\sin^2 2\vartheta_{ee})_{\rm b.f.}$	0.017	0.019	0.017	0.017
$(\Delta m^2_{41})_{\rm b.f.}/{\rm eV}^2$	1.32	1.32	1.32	1.32
$\Delta\chi^2_{4\nu\text{-}3\nu}$	10.1	10.3	9.1	9.3
$n\sigma_{4\nu\text{-}3\nu}$	2.7	2.8	2.6	2.6

Table 1. Results of the global ν_e and $\bar{\nu}_e$ disappearance fits obtained using NEOS/Daya Bay (RSRF(N/DB)) or NEOS/RENO (RSRF(N/R)) data. The column titles HM, HKSS, EF, and KI refer to the four reactor neutrino fluxes discussed in Section 3. The tables show the minimum value $\chi^2_{\rm min}$ of χ^2, the goodness of fit (GoF), the best-fit values of $\sin^2 2\vartheta_{ee}$ and Δm^2_{41}, the χ^2 difference $\Delta\chi^2_{4\nu\text{-}3\nu}$ between the 3+1 4ν fit and the 3ν fit, and the statistical significance ($n\sigma_{4\nu\text{-}3\nu}$) of the corresponding indication in favor of 3+1 4ν mixing.

indication in favor of 3+1 active-sterile neutrino mixing in the global fits with the NEOS/Daya Bay data. The indication decreases to 2.6–2.8σ if the NEOS/RENO are used. The values of the best-fit points are in all cases around $\sin^2 2\vartheta_{ee} \simeq 0.02$ and $\Delta m^2_{41} \simeq 1.3\ {\rm eV}^2$.

Figure 3 shows the 2σ and 3σ allowed regions in the $(\sin^2 2\vartheta_{ee}, \Delta m^2_{41})$ plane obtained from the global fits with different neutrino flux models and considering either the NEOS/Daya Bay [37] spectral ratio (Figs. 3(a) and 3(c)) or the NEOS/RENO [38] spectral ratio (Figs. 3(b) and 3(d)).

The restrictions of the solar neutrino constraint increase the tension with the results of the Gallium experiments in the framework of 3+1 active-sterile neutrino mixing. From Tab. 8 of Ref. [22], one can see that the global fit gives values of parameter goodness of fit that are well below 1% for all the fits with different data combinations.

In Fig. 3 one can notice the curious approximate coincidence of the values of Δm^2_{41} for the global best-fit points ($(\Delta m^2_{41})_{\rm b.f.} = 1.3\,{\rm eV}^2$) and the Gallium best-fit points ($(\Delta m^2_{41})_{\rm b.f.} = 1.3\,{\rm eV}^2$ for Bahcall, Kostensalo and Semenov, and $(\Delta m^2_{41})_{\rm b.f.} = 1.2\,{\rm eV}^2$ for Ground State). This coincidence has no meaning in the framework of 3+1 active-sterile neutrino mixing, because the best-fit values of the unique mixing parameter $\sin^2 2\vartheta_{ee}$ are too different and the 3σ allowed regions are well separated for $\Delta m^2_{41} \approx 1.3\,{\rm eV}^2$.

6 Summary and conclusions

We have discussed in a systematic way the results of ν_e and $\bar{\nu}_e$ disappearance experiments which are relevant for the hypothetical existence of short-baseline neutrino oscillations due to 3+1 active-sterile neutrino mixing. We started in Section 2 with the analysis of the results of the Gallium source experiments, motivated by the recent results of the BEST experiment [5, 6], which revived the Gallium Anomaly confirming the results of the GALLEX [13–15] and SAGE [10, 16–18] experiments. We have shown that the explanation of the Gallium Anomaly in the framework of 3+1 active-sterile neutrino mixing requires rather large values of the mixing between ν_e and the new massive neutrino ν_4 for all the cross section models of neutrino detection in the Gallium source experiments. This means that ν_4 is not almost entirely sterile, as it would be required for considering 3+1 active-sterile mixing as a perturbation of standard three-neutrino mixing. This is required for the explanation of the neutrino oscillations observed in solar, atmospheric and long-baseline neutrino oscillation experiments.

We also considered the results of reactor neutrino experiments and we presented the results of 3+1 fits of the measured rates and the ratios of spectra measured at different distances. In Section 3, we have shown that the measured reactor rates imply upper bounds for active-sterile mixing that are in tension with the results of the Gallium experiments for all the cross section models of neutrino detection in the Gallium source experiments and all the reactor neutrino flux models.

In Section 4, we presented the results of a global fit of the most recent available data of the reactor neutrino experiments which measured the ratio of the neutrino spectra at different distances in order to probe neutrino oscillations independently from the absolute values of the neutrino fluxes. We have shown that the results depend significantly on the choice to consider either the NEOS/Daya Bay [37] or NEOS/RENO [38] spectral ratio data. In the case of the NEOS/Daya Bay, there is a 3.1σ indication in favor of short-baseline oscillations with best-fit parameter values $\sin^2 2\vartheta_{ee} = 0.022$ and $\Delta m^2_{41} = 1.29\,{\rm eV}^2$, which is driven by the overlap of the surrounding allowed regions of NEOS/Daya Bay and DANSS [32]. On the other hand, the overlap of the NEOS/RENO and DANSS allowed regions is smaller and leads to an indication in favor of short-baseline oscillations of only 2.6σ with best-fit parameters values $\sin^2 2\vartheta_{ee} = 0.017$ and $\Delta m^2_{41} = 1.32\,{\rm eV}^2$. Although the NEOS/RENO comparison may be favored by the smaller systematic uncertainties which were estimated by the NEOS and RENO collaborations using the fact that the two experiments detect neutrino fluxes from similar reactors in the same complex, we think that we cannot dismiss the NEOS/Daya Bay data, which should be considered as a different measurement based on the Daya Bay neutrino flux measurement. Since we cannot combine the two measurements because the NEOS data would be double counted, we remain with the ambiguity of the two different results which hopefully will be solved by future measurements.

We have also shown that the results of the reactor spectral ratio experiments are in tension with the neutrino oscillation explanation of the Gallium Anomaly and the tension is stronger when the NEOS/Daya Bay data are con-

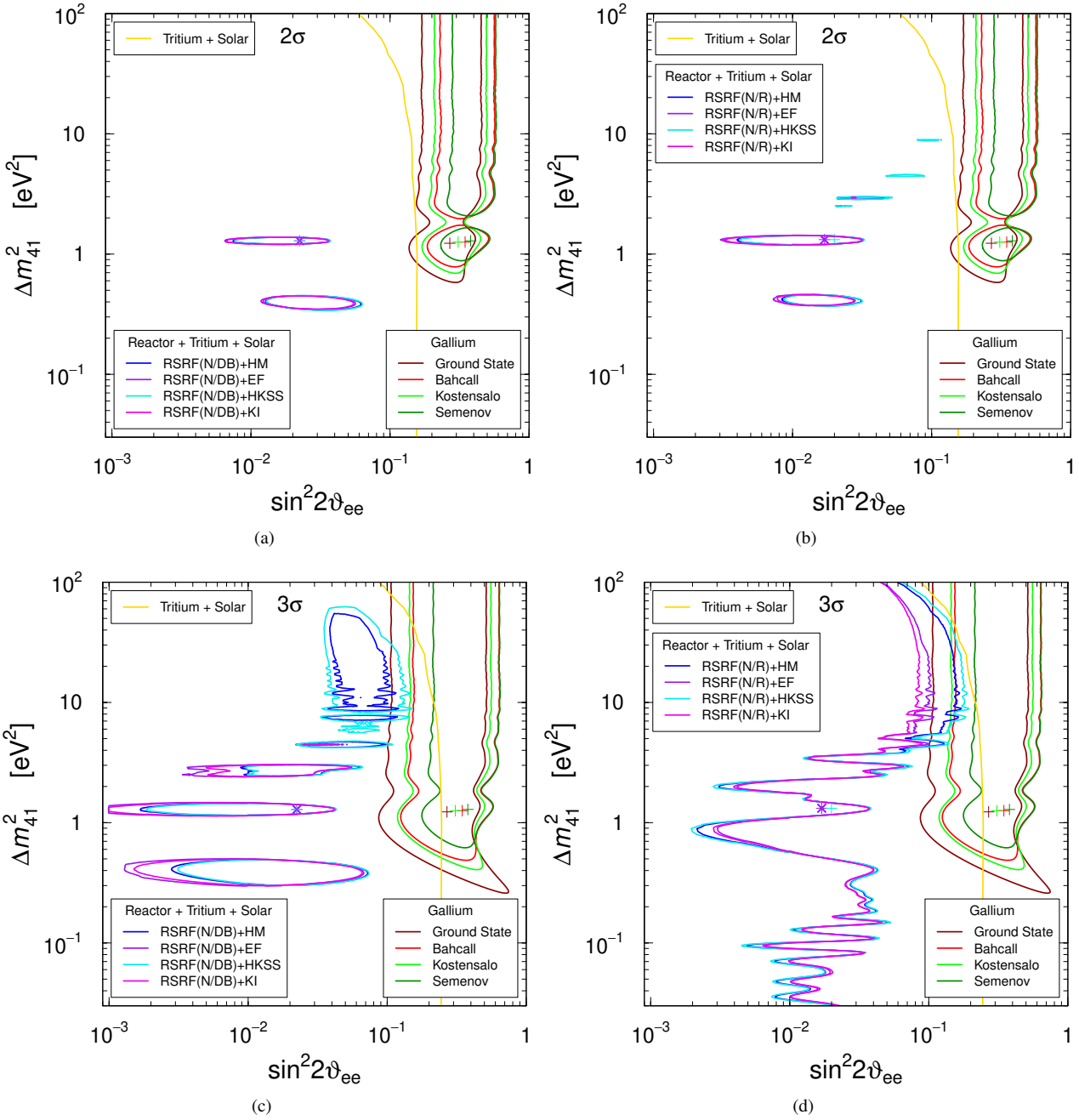

Figure 3. Comparison of the contours delimiting the [(a) and (b)] 2σ and [(c) and (d)] 3σ allowed regions in the $(\sin^2 2\vartheta_{ee}, \Delta m^2_{41})$ plane obtained from the combined analysis of the data of the reactor rate experiments with different flux models, the spectral ratio experiments,reactor the Tritium experiments, and the solar bound with those obtained from the Gallium data with different cross sections. Also shown is the 3σ bound obtained from the combination of the Tritium and solar bounds. The figures differ by the use of [(a) and (c)] NEOS/Daya Bay [37] or [(b) and (d)] NEOS/RENO [38] spectral ratio data. The best-fit points are indicated by crosses.

sidered, with about 0.15% parameter goodness of fit for all the Gallium detection cross section models, whereas considering the NEOS/RENO data we obtain about 1.3%. Finally, we discussed in Section 5 the results of the global fit of the ν_e and $\bar{\nu}_e$ disappearance data. We have shown that the tension is dramatic in the case of the global fit, with values of the parameter goodness of fit well below 1% for all the cases with different data choices (NEOS/Daya Bay or NEOS/RENO), different reactor flux models, and different Gallium detection cross sections.

In conclusion, we think that the results presented in Ref. [22] show the present status of our knowledge on short-baseline ν_e and $\bar{\nu}_e$ disappearance in the framework of 3+1 active-sterile neutrino mixing and the dramatic tension between the the neutrino oscillation explanation of the Gallium Anomaly and the results of the other experiments. We conclude that it is very likely that the Gallium Anomaly is not due to neutrino oscillations and some other explanation must be found.

Acknowledgments

Work supported by the research grant "The Dark Universe: A Synergic Multimessenger Approach" number 2017X7X85K under the program "PRIN 2017" funded by the Italian Ministero dell'Istruzione, Università e della Ricerca (MIUR). C.A.T. also acknowledges support from *Departments of Excellence* grant awarded by MIUR and the research grant *TAsP (Theoretical Astroparticle Physics)* funded by Istituto Nazionale di Fisica Nucleare (INFN).

References

[1] C. Giunti, T. Lasserre, Ann. Rev. Nucl. Part. Sci. **69**, 163 (2019), arXiv:1901.08330
[2] A. Diaz, C. Arguelles, G. Collin, J. Conrad, M. Shaevitz, Phys.Rept. **884**, 1 (2020), arXiv:1906.00045
[3] S. Boser, C. Buck, C. Giunti, J. Lesgourgues, L. Ludhova, S. Mertens, A. Schukraft, M. Wurm, Prog.Part.Nucl.Phys. **111**, 103736 (2020), arXiv:1906.01739
[4] B. Dasgupta, J. Kopp, Phys.Rept. **928**, 63 (2021), arXiv:2106.05913
[5] V. Barinov et al. (BEST), Phys.Rev.Lett. **128**, 232501 (2022), arXiv:2109.11482
[6] V.V. Barinov et al. (2022), 2201.07364
[7] P.F. de Salas, D.V. Forero, S. Gariazzo, P. Martinez-Mirave, O. Mena, C.A. Ternes, M. Tortola, J.W.F. Valle, JHEP **2021**, 071 (2020), arXiv:2006.11237
[8] J.M. Berryman, P. Huber, JHEP **2101**, 167 (2021), arXiv:2005.01756
[9] C. Giunti, Y. Li, C. Ternes, Z. Xin, Phys.Lett.B **829**, 137054 (2022), arXiv:2110.06820
[10] J.N. Abdurashitov et al. (SAGE), Phys. Rev. **C73**, 045805 (2006), nucl-ex/0512041
[11] M. Laveder, Nucl. Phys. Proc. Suppl. **168**, 344 (2007)
[12] C. Giunti, M. Laveder, Mod. Phys. Lett. **A22**, 2499 (2007), hep-ph/0610352
[13] P. Anselmann et al. (GALLEX), Phys. Lett. **B342**, 440 (1995)
[14] W. Hampel et al. (GALLEX), Phys. Lett. **B420**, 114 (1998)
[15] F. Kaether, W. Hampel, G. Heusser, J. Kiko, T. Kirsten, Phys. Lett. B **685**, 47 (2010), 1001.2731
[16] J.N. Abdurashitov et al. (SAGE), Phys. Rev. Lett. **77**, 4708 (1996)
[17] J.N. Abdurashitov et al. (SAGE), Phys. Rev. **C59**, 2246 (1999), hep-ph/9803418
[18] J.N. Abdurashitov et al. (SAGE), Phys. Rev. C **80**, 015807 (2009), 0901.2200
[19] J.N. Bahcall, Phys. Rev. **C56**, 3391 (1997), hep-ph/9710491
[20] J. Kostensalo, J. Suhonen, C. Giunti, P.C. Srivastava, Phys.Lett. **B795**, 542 (2019), arXiv:1906.10980
[21] S.V. Semenov, Phys. Atom. Nucl. **83**, 1549 (2020)
[22] C. Giunti, Y.F. Li, C.A. Ternes, O. Tyagi, Z. Xin, JHEP **10**, 164 (2022), 2209.00916
[23] C. Giunti, Y.F. Li, C.A. Ternes, Z. Xin (2022), 2212.09722
[24] G. Mention et al., Phys. Rev. **D83**, 073006 (2011), arXiv:1101.2755
[25] T.A. Mueller et al., Phys. Rev. **C83**, 054615 (2011), arXiv:1101.2663
[26] P. Huber, Phys. Rev. **C84**, 024617 (2011), arXiv:1106.0687
[27] L. Hayen, J. Kostensalo, N. Severijns, J. Suhonen, Phys.Rev. **C100**, 054323 (2019), arXiv:1908.08302
[28] M. Estienne, M. Fallot et al., Phys. Rev. Lett. **123**, 022502 (2019), arXiv:1904.09358
[29] V. Kopeikin, M. Skorokhvatov, O. Titov, Phys. Rev. D **104**, L071301 (2021), 2103.01684
[30] M. Maltoni, T. Schwetz, Phys. Rev. **D68**, 033020 (2003), hep-ph/0304176
[31] I. Alekseev et al. (DANSS), Phys.Lett. **B787**, 56 (2018), arXiv:1804.04046
[32] M. Danilov (2022), talk presented at ICHEP 2022, 41th International Conference on High Energy Physics, 6-13 July 2022, Bologna, Italy
[33] J. Ashenfelter et al. (PROSPECT), Phys.Rev.Lett. **121**, 251802 (2018), arXiv:1806.02784
[34] M. Andriamirado et al. (PROSPECT), Phys.Rev. **D103**, 032001 (2021), arXiv:2006.11210
[35] H. Almazan et al. (STEREO), Phys.Rev.Lett. **121**, 161801 (2018), arXiv:1806.02096
[36] H. Almazan Molina et al. (STEREO), Phys.Rev. **D102**, 052002 (2020), arXiv:1912.06582
[37] Y. Ko et al. (NEOS), Phys.Rev.Lett. **118**, 121802 (2017), arXiv:1610.05134
[38] Z. Atif et al. (RENO, NEOS), Phys. Rev. D **105**, L111101 (2022), arXiv:2011.00896
[39] F. An et al. (Daya Bay), Chin.Phys. **C41**, 013002 (2017), arXiv:1607.05378
[40] A. Serebrov et al., Phys.Rev.D **104**, 032003 (2021), arXiv:2005.05301
[41] M. Danilov, J.Phys.Conf.Ser. **1390**, 012049 (2019), arXiv:1812.04085
[42] M. Andriamirado et al. (PROSPECT, STEREO) (2020), 2006.13147
[43] M.V. Danilov, N.A. Skrobova, JETP Lett. **112**, 452 (2020)
[44] C. Giunti, Y.F. Li, C.A. Ternes, Y.Y. Zhang, Phys. Lett. B **816**, 136214 (2021), 2101.06785